A VISCOPLASTIC CONSTITUTIVE THEORY FOR METAL MATRIX COMPOSITES AT HIGH TEMPERATURE

David N. Robinson*
The University of Akron
Akron, Ohio 44325

Stephen F. Duffy*
Cleveland State University
Cleveland, Ohio 44115

John R. Ellis†
The University of Akron
Akron, Ohio 44325

SUMMARY

A viscoplastic constitutive theory is presented for representing the high-temperature deformation behavior of metal matrix composites. The point of view taken is one of a continuum wherein the composite is considered a material in its own right, with its own properties that can be determined for the composite as a whole. It is presumed that a single preferential (fiber) direction is identifiable at each material point (continuum element), thereby admitting the idealization of local transverse isotropy. A key ingredient in this work is the specification of an experimental program for the complete determination of the material functions and parameters for characterizing a particular metal matrix composite. The parameters relating to the strength of anistropy can be determined through tension and torsion tests on longitudinally and circumferentially reinforced thin-walled tubes. Fundamental aspects of the theory are explored through a geometric interpretation of some basic features analogous to those of the classical theory of plasticity.

E-3956-2

INTRODUCTION

Structural alloys used in high-temperature applications exhibit complex thermomechanical behavior that is inherently time-dependent and hereditary, in the sense that current behavior depends not only on current conditions but also on thermomechanical history. Considerable attention is being focused now on metal matrix composite materials that possess strong directional characteristics. In high-temperature applications these materials exhibit all the complexities of conventional alloys (e.g., creep, relaxation, recovery, rate sensitivity, etc.), and in addition, their strong initial anistropy adds further complexities.

Here, we present a continuum theory to represent the high-temperature, time-dependent, hereditary deformation behavior of materials that are initially

*NASA Lewis Resident Research Associate.
†Now at NASA Lewis.

transversely isotropic. The theory is intended to apply to materials, particularly metallic composites, that can be idealized as psuedohomogeneous continua with locally definable directional characteristics.

The composite material is viewed as a material in its own right, with its own properties that can be measured and specified for the composite as a whole. Experiments for this purpose are outlined in detail in the fourth section of the paper. This view is intended to satisfy the structural analyst or design engineer who needs reasonably simple continuum methods of structural analysis to predict deformation behavior in complex multiaxial situations, particularly at high temperature where material response is enormously complex. Indeed, the prediction of component lifetime depends critically on the accurate prediction of deformation behavior.

The alternative approach is concerned with detailed interactions of the constituents of the composite: fabrication, bonding, and the relation of the properties of the composite to the individual properties of the fiber and matrix. Clearly, such problems are of great importance, and the two approaches mentioned are not mutually exclusive. Here, however, the continuum point of view will be emphasized. This is done in the same spirit that the theories of elasticity, plasticity, viscoelasticity, and others are formulated; on the basis of macroscopic observations, without direct consideration of the details of intermolecular, intergranular or interdislocation interactions. Of course, this is not to imply that qualitative (and quantitative) understanding of behavior on the microscale should not strongly influence the formulation and structure of phenomenological theories.

The authors are hopeful this research will complement other ongoing efforts at NASA Lewis Research Center relating to the high-temperature behavior of metal matrix composites (refs. 1 to 5). Parts of the present work (believed essential in representing the time-dependent, hereditary behavior of metals) may prove helpful in extending the micromechanics equations for the thermal and mechanical behavior of composites (refs. 1 and 2) to include some important viscoplastic features.

STATEMENT OF THE THEORY

This work is an extension of that by Robinson (ref. 6) and includes the former work as a special case. In reference 6, three material parameters over and above those necessary for representing isotropic viscoplastic behavior were necessary to account for transverse isotropy. Here, four parameters have to be specified (fig. 1). The additional parameter arises from a less restrictive set of assumptions made in the theoretical development. Definition of the additional parameter leads to more testing to characterize a particular material but, at the same time, offers the distinct advantage of greater flexibility in correlating predictions with experimental data.

As in reference 6, the starting point is the assumed existence of a dissipation potential function (refs. 7 to 9); that is

$$\Omega = \Omega\ (\sigma_{ij}, \alpha_{ij}, T) \tag{1}$$

with the generalized normality structure

$$\dot{\varepsilon}_{ij} = \frac{\partial \Omega}{\partial \sigma_{ij}} \tag{2}$$

$$\frac{-\dot{\alpha}_{ij}}{h(\alpha_{kl})} = \frac{\partial \Omega}{\partial \alpha_{ij}} \tag{3}$$

Here, σ_{ij} and α_{ij} denote the components of the applied and internal stress tensors, respectively, $\dot{\varepsilon}_{ij}$ denotes the components of the inelastic strain rate tensor, h is a scalar function of the internal stress, and T is the temperature. Although Ω is shown as a function of temperature, only isothermal deformations will be considered in the following development. Extension to nonisothermal conditions follows as in reference 10.

In the fully isotropic case, the stress dependence of Ω enters only through the principal invariants of the deviatoric applied and internal stresses (ref. 10). For transverse isotropy, Ω must depend additionally on the local preferential (fiber) direction denoted by the components of a unit vector d_i (or, as the sense of d_i is immaterial, on the components of a symmetric directional tensor $d_i d_j$). Form invariance (objectivity) of Ω requires that it depend only on invariants of the applied and internal stresses, the directional tensor, and certain products of these tensors (ref. 11).

A subset of the irreducible set of invariants for form invariance (integrity basis) is used (ref. 11)

$$I_1 = \frac{1}{2}\sum_{ij}\sum_{ji} \tag{4}$$

$$I_2 = d_i d_j \sum_{jk}\sum_{ki} - 4I_3^2 \tag{5}$$

$$I_3 = \frac{1}{2}\, d_i d_j \sum_{ji} \tag{6}$$

where Σ_{ij} denotes the components of the effective stress, that is, the difference of the deviatoric applied and internal stresses. I_1 relates, as in the isotropic case, to the effective octahedral shear stress, I_2 relates to the shear component of the effective traction on the plane of isotropy (plane normal to d_i), and I_3 corresponds to the normal component of the effective traction along d_i.

Taking Ω to be dependent on the appropriate invariants and using equations (2) and (3), the flow law becomes

$$\dot{\varepsilon}_{ij} = f(F)\left\{\sum_{ij} - \left(\frac{\eta^2 - 1}{\eta^2}\right)\left(d_k d_i \sum_{jk} + d_j d_k \sum_{ki} - 4I_3 d_i d_j\right) - 4I_3\left(\frac{\omega^2 - 1}{4\omega^2 - 1}\right)\left(3d_i d_j - \delta_{ij}\right)\right\} \tag{7}$$

and the evolutionary law becomes

$$\dot{a}_{ij} = \frac{H}{G^{\beta}}\dot{\varepsilon}_{ij} - RG^{m-\beta}\left\{a_{ij} - \left(\frac{\eta^2 - 1}{\eta^2}\right)\left(d_k d_i a_{jk} + d_j d_k a_{ki} - 4I_3' d_i d_j\right) - 4I_3'\left(\frac{\omega^2 - 1}{4\omega^2 - 1}\right)\left(3d_i d_j - \delta_{ij}\right)\right\} \tag{8}$$

with

$$F = \frac{1}{K_T^2}\left\{I_1 - \left(\frac{\eta^2 - 1}{\eta^2}\right)I_2 - \left(\frac{12(\omega^2 - 1)}{4\omega^2 - 1} I_3^2\right) - 1\right\} \tag{9}$$

and

$$G = \frac{1}{K_T^2}\left\{I_1' - \left(\frac{\eta^2 - 1}{\eta^2}\right)I_2' - \left(\frac{12(\omega^2 - 1)}{4\omega^2 - 1}\right)(I_3')^2\right\} \tag{10}$$

The function $f(F)$ and the material parameters m, β, R, H, and K_T are associated with the viscoplastic response (ref. 10); the components of the unit vector d_i (specified in terms of two Euler angles), ω, and η, are the four parameters associated with the direction and strength of transverse isotropy (fig. 1). I_1', I_2', I_3' are invariants of the deviatoric internal stress a_{ij}, similar in form to equations (4) to (6). Note that with $\omega = \eta = 1$ equations (7) to (10) reduce to the isotropic forms reported in reference 10. The details of the derivation of equations (7) to (10) are left to the references 6, 10, and 11.

For a particular composite material the parameters ω and η, designating the strength of anisotropy, depend on the individual constituent materials (fiber and matrix) and their volume ratio. Different volume ratios involving the same constituents are considered different materials. In extending the present theory to arbitrarily large deformations, the local volume ratio may change in the course of deformation (as does the local density in an isotropic material); in which case evolutionary laws for ω and η must be specified. Also, for large deformations and/or rotations, the preferential direction d_i may convect with the material thereby resulting in increasing anisotropic inhomogeneity. At this time, large deformations and rotations are not considered.

SOME FUNDAMENTAL IMPLICATIONS OF THE THEORY

As in earlier works (refs. 6 and 10) F plays the role of a Bingham-Prager threshold stress function; inelastic response occurs only for $F > 0$. The surface $F = 0$ in the stress space encloses stress states that produce elastic behavior only. Figure 2 shows a typical projection of $F = 0$ on the $\sigma_{11} - \sigma_{22}$ plane for full isotropy ($\omega = \eta = 1$) and the virgin state ($a_{ij} \simeq 0$). An infinite family of surfaces $F =$ constant is associated with each inelastic state. The direction of the inelastic strain rate vector at each stress point on a given surface is directed normal to the surface. The existence of these surfaces and the concept of normality has been demonstrated experimentally for the isotropic case in reference 12.

Figure 3 shows the corresponding projection of $F = 0$ on the $\sigma_{11} - \sigma_{22}$ plane for the transversely isotropic case with $\omega = \eta = 2$. For each curve shown, the preferential direction is taken to lie in the X_1, X_2 physical plane with a specified angle φ relative to the X_1 axis. These curves, as in figure 2, correspond to the virgin state. The shape and orientation of the surfaces $F = 0$ (and all surfaces $F =$ constant) now depend on the local preferential direction d_i. Note, for instance, that for $\varphi = 0$, the intercept on the σ_{11} axis is the threshold stress Y_L, (figs. 1 and 3), the intercept on the σ_{22} axis is Y_T, and $\omega = (Y_L/Y_T) = 2$.

As an interesting and illustrative example, consider the stress path $\sigma_{11} = 2\sigma_{22}$ that is denoted as a dotted line in figures 2 and 3. This is equivalent to the stress state in a thin-walled tube with closed ends under internal pressure, where σ_{11} is the circumferential or hoop stress and σ_{22} the axial stress. With increasing pressure, the stress point eventually reaches the surface $F = 0$ and the tube begins to deform inelastically. In figure 2, corresponding to the isotropic tube, inelastic deformation occurs as indicated by the strain rate vector shown. Normality dictates that the axial strain rate $\dot{\varepsilon}_{22}$ is zero, that is, the tube incurs no inelastic change in length. Contrast this behavior with that of figure 3 with $\varphi = 0$. This case represents a circumferentially reinforced tube with a threshold stress in the circumferential direction that is twice that of the axial direction. As $F = 0$ is reached and inelasticity begins to occur, the (normal) strain rate vector has a relatively large axial component $\dot{\varepsilon}_{22}$. The thin tube now experiences inelastic axial extension. Thus the mode of inelastic deformation has changed qualitatively with reinforcement. Similar observations are well documented for time-independent reinforced structures (ref. 13).

EXPERIMENTAL DETERMINATION OF MATERIAL PARAMETERS

Two types of specimens are presumed to be available: thin-walled composite tubes that are longitudinally reinforced (having a single fiber direction oriented axially) and those that are circumferentially reinforced (circumferential fiber orientation). Each type of tube will be loaded either in pure torsion or in pure tension. Although not discussed here, combined tension and torsion experiments can be used as verification tests to assess the correctness of the multiaxial theory (ref. 12). As is well known, the thin-walled

tube is an ideal specimen for the development of constitutive relationships in that it provides a nearly homogeneous and uniform region of stress and strain, and is statically determinate.

Those parameters relating to the strength of anisotropy, ω and η, and the threshold strength $Y_L(\equiv K_T(4\omega^2 - 1)^{1/2})$ are determined through probing tests. These tests are designed to determine the inelastic strain rate for a given stress in the neighborhood of a constant inelastic state, here the initial (virgin) state of the material. Indeed, it is the degree of initial transverse isotropy that is of interest in this study. The probing test, conducted properly, furnishes the desired information without significantly changing the state.

The material function $f(F)$ and the parameters m, β, R, and H relating to the viscoplastic properties of the composite are obtained from a combination of the probing tests and creep tests conducted on longitudinally-reinforced tubes (or bars). Alternately, in place of the latter tests, one could use torsion tests on circumferentially reinforced tubes as outlined in reference 11. The present choice of basing the viscoplastic parameters on uniaxial creep tests of axially reinforced tubes is motivated by (1) the relative ease of fabricating longitudinally reinforced tubular specimens over those reinforced circumferentially and (2) the advantage of characterizing directly the inelastic response in the critical fiber direction. In the case of extreme reinforcement (e.g., a relatively high volume ratio of very strong fibers that remain essentially elastic), composite structures are known to be "shear limited" (ref. 12), and their inelastic behavior is governed largely by the shear response of the matrix. Under these conditions it may be advantageous to determine the viscoplastic parameters through the torsional creep tests on circumferentially reinforced tubes discussed in reference 11.

First, consider a probing test on a longitudinal tube. Pure torsion and pure tension probes are schematically illustrated as the respective paths o-a and o-b in the σ-τ stress space of figure 4(a). Data from such tests take the form of a sequence of stress and inelastic strain rate pairs, $(\tau,\dot{\gamma})$ along o-a and $(\sigma,\dot{\varepsilon})$ along o-b. These data can be conveniently plotted as the solid curves σ versus $\dot{\varepsilon}$ and τ versus $\dot{\gamma}$ in figure 5. Extrapolation of the σ versus $\dot{\varepsilon}$ curve in figure 5 to the $\dot{\varepsilon} = 0$ axis furnishes the longitudinal threshold stress Y_L.

Specialization of equations (9) and (7) for the path o-a in figure 4(a) results in

$$F = \frac{\tau^2}{\eta^2 K_T^2} - 1 \tag{11}$$

and

$$2\dot{\varepsilon}_{12} = \dot{\gamma} = f(F)\,\frac{2\tau}{\eta^2} \tag{12}$$

in which $\tau(\equiv\sigma_{12})$ is the applied shear stress. The corresponding equations for path o-b are

$$F = \frac{\sigma^2}{(4\omega^2 - 1)K_T^2} - 1 \tag{13}$$

and

$$\dot{\varepsilon}_{11} = \dot{\varepsilon} = f(F)\,\frac{2\sigma}{4\omega^2 - 1} \tag{14}$$

where $\sigma(\equiv\sigma_{11})$ is the applied normal stress. Now for F = constant (Ω = constant), equations (11) and (13) give

$$\frac{\sigma}{\tau} = \left(\frac{4\omega^2 - 1}{\eta^2}\right)^{1/2} \tag{15}$$

while equations (12) and (14) combine to give

$$\frac{\dot{\gamma}}{\varepsilon} = \left(\frac{4\omega^2 - 1}{\eta^2}\right)\frac{\tau}{\sigma} = \frac{\sigma}{\tau} \tag{16}$$

or

$$\sigma\dot{\varepsilon} = \tau\dot{\gamma} \tag{17}$$

Thus, in figure 4(a) points $(\tau,\dot{\gamma})$ along o-a and $(\sigma,\dot{\varepsilon})$ along o-b, having the same dissipation rate, lie on a common F = constant (Ω = constant) curve; for example, the particular points $(\tau_A, \dot{\gamma}_A)$ and $(\sigma_A,\dot{\varepsilon}_A)$ in figure 4(b).

Pairs of points in the plot of figure (5) that lie on an F = constant locus are related geometrically such that areas $\sigma_A\dot{\varepsilon}_A$ and $\tau_A\dot{\gamma}_A$ are equal. Several such pairs can be matched up giving an average value of the ratio

$$\frac{\sigma}{\tau} = \left(\frac{\sigma}{\tau}\right)_L \tag{18}$$

Thus, from equation (15)

$$\left(\frac{4\omega^2 - 1}{\eta^2}\right)^{1/2} = \left(\frac{\sigma}{\tau}\right)_L \tag{19}$$

Probing tests on circumferentially reinforced tubes produce results entirely analogous to those discussed above for longitudinally reinforced tubes; counterparts of figures 4(a), 4(b), and 5 can be constructed.

The governing equations corresponding to the pure torsional loading of the circumferential tube are identical to equations (11) and (12). The equations relating to pure tension of the circumferential tube are

$$F = \frac{\sigma^2\omega^2}{(4\omega^2 - 1)K_T^2} - 1 \tag{20}$$

and

$$\dot{\varepsilon}_{11} = \dot{\varepsilon} = f(F)\,\frac{2\sigma}{4\omega^2 - 1}\,\omega^2 \tag{21}$$

As before, for F = constant (Ω = constant), equations (11) and (20) combine to give

$$\frac{\sigma}{\tau} = \left(\frac{4\omega^2 - 1}{\eta^2\omega^2}\right)^{1/2} \tag{22}$$

whereas equations (12) and (21) give

$$\frac{\dot{\gamma}}{\varepsilon} = \left(\frac{4\omega^2 - 1}{\eta^2\omega^2}\right)\frac{\tau}{\sigma} = \frac{\sigma}{\tau} \tag{23}$$

or

$$\sigma\dot{\varepsilon} = \tau\dot{\gamma} \tag{24}$$

Again, in figure 4(a) points $(\tau,\dot{\gamma})$ along o-a and $(\sigma,\dot{\varepsilon})$ along o-b, with equal dissipation rates, fall on a common F = constant curve (fig. 4(b)). Similarly, matching pairs of points corresponding to F = constant curves and averaging gives

$$\left(\frac{4\omega^2 - 1}{\omega^2\eta^2}\right)^{1/2} = \left(\frac{\sigma}{\tau}\right)_C \tag{25}$$

Making use of equation (19), from tests on longitudinally reinforced tubes, and equation (25), from circumferentially reinforced tubes, results in

$$\omega = \frac{\left(\frac{\sigma}{\tau}\right)_L}{\left(\frac{\sigma}{\tau}\right)_C} \tag{26}$$

and

$$\eta = \frac{(4\omega^2 - 1)^{1/2}}{\left(\frac{\sigma}{\tau}\right)_L} \tag{27}$$

thereby completely characterizing the strength of initial anisotropy. Recall that the longitudinal threshold stress $Y_L(\equiv K_T(4\omega^2 - 1)^{1/2})$ is also known.

Turn now to the determination of the remaining viscoplastic material parameters. As indicated earlier, although several options are open in this regard (including torsional tests on circumferentially strengthened tubes as in ref. 11), the choice here is to consider uniaxial creep tests on longitudinally reinforced thin-walled tubes. This is in addition to the probing tests on longitudinal tubes already discussed. Typical results of uniaxial creep tests are illustrated in figure 6.

According to the present theory, the governing equations for the considered creep conditions are

$$F = \frac{(\sigma - s)^2}{Y_L^2} - 1 \tag{28}$$

$$G = \frac{s^2}{Y_L^2} \tag{29}$$

$$\dot{\varepsilon} = \frac{1}{\mu(4\omega^2 - 1)} F^n(\sigma - s) \tag{30}$$

and

$$\dot{s} = \left(\frac{\hat{H}}{s^{\hat{\beta}}}\right)\dot{\varepsilon} - \hat{R}s^{\hat{m}-\hat{\beta}+1} \tag{31}$$

where

$$\left.\begin{aligned} f(F) &= \frac{F^n}{2\mu} \\ \hat{H} &= \frac{3HY_L^{2\beta}}{2} \\ \hat{R} &= \frac{3R}{(4\omega^2 - 1)Y_L^{2(m-\beta)}} \\ \hat{\beta} &= 2\beta \\ \hat{m} &= 2m \end{aligned}\right\} \tag{32}$$

Here, $\dot{\varepsilon}(\equiv \dot{\varepsilon}_{11})$ is the axial component of inelastic strain rate, and $s(\equiv \alpha_{11})$ is the uniaxial component of the internal state variable α_{ij}. The first of equations (32) indicates that the function $f(F)$ has been specialized as a power function characterized by the constants μ and n.

Note for future reference that for $F \gg 0$, equation (30), the flow law, can be approximated as

$$\dot{\varepsilon} \simeq B(\sigma - s)^{2n+1} \tag{33}$$

where

$$B = \frac{1}{\mu(4\omega^2 - 1)Y_L^{2n}} \tag{34}$$

Also, during the early part of primary (transient) creep where s is small (fig. 6), the evolutionary law equation (31) can be approximated as

$$\dot{s} \simeq \left(\frac{\hat{H}}{\hat{s}^{\hat{\beta}}}\right)\dot{\varepsilon} \tag{35}$$

The initial creep rate following abrupt application of the stress σ (fig. 6), is expressed by equation (33) with $s \simeq 0$. That is

$$\dot{\varepsilon} = B\sigma^{2n+1} \tag{36}$$

Information for determining B and n can be obtained directly from the initial creep rates as illustrated in figure 6, or alternatively, and more accurately, from the data generated from the probing tests already considered; the σ versus $\dot{\varepsilon}$ data illustrated in figure 5. By assuming these data correlate with equation (36), a plot of $\log(\dot{\varepsilon})$ versus $\log(\sigma)$ provides both n and B directly (fig. 7). If correlation with equation (36) is not satisfactory a different function $f(F)$ may have to be considered in the first of equations (32). In this study, it is assumed that the power law form is appropriate (as has been found for several isotropic alloys) and that n and B can be determined. With n, B, ω, and Y_L known, μ is then determined from equation (34).

Now focus attention on steady state creep information (fig. 6). At steady state $\dot{s} = 0$, so from equation (31)

$$\dot{\varepsilon}_s = \left(\frac{\hat{R}}{\hat{H}}\right) s_s^{\hat{m}+1} \tag{37}$$

Steady state creep data provides the pairs $(\sigma, \dot{\varepsilon}_s)$ but with ω, μ, Y_L, and n known, equation (30) allows s_s (the steady state internal stress) to be calculated for each pair, thus giving the data pairs $(\dot{\varepsilon}_s, s_s)$. Plotting $\log(\dot{\varepsilon}_s)$ versus $\log(s_s)$ provides values of $(\hat{R}/\hat{H})$ and $\hat{m}$ directly as indicated by the logarithmic form of equation (37) and figure 8. The last of equations (32) provides the exponent m.

Attention is now turned to the primary creep stage of the creep tests. As indicated in equation (35), the evolution of s in the early stages of primary creep is governed by

$$\dot{s} \simeq \left(\frac{\hat{H}}{s^{\hat{\beta}}}\right)\dot{\varepsilon} \tag{38}$$

Eliminating time and integrating

$$\int_{s\simeq 0}^{s} s^{\hat{\beta}}\, ds = \int_{0}^{\varepsilon} \hat{H}\, d\varepsilon \tag{39}$$

results in

$$\frac{s^{\hat{\beta}+1}}{(\hat{\beta}+1)} = \hat{H}\varepsilon \tag{40}$$

or in transposed logarithmic form

$$\log(\varepsilon) = (\hat{\beta}+1)\log(s) + \log\left(\frac{1}{\hat{H}(\hat{\beta}+1)}\right) \tag{41}$$

Now using equation (33) to solve for s yields,

$$s = \sigma - \left(\frac{\dot{\varepsilon}}{B}\right)^{1/2n+1} \tag{42}$$

and substituting this result into equation (41) gives

$$\log(\varepsilon) = (\hat{\beta}+1)\log\left\{\sigma - \left(\frac{\dot{\varepsilon}}{B}\right)^{1/2n+1}\right\} + \log\left(\frac{1}{\hat{H}(\hat{\beta}+1)}\right) \tag{43}$$

Early primary creep data provides the data triplets $(\sigma,\varepsilon,\dot{\varepsilon})$ at each time. With B and n known, these data can be plotted (fig. 9) in the form of equation (43) yielding $\hat{H}(\hat{\beta}+1)$ and $(\hat{\beta}+1)$. Using equations (32), β and H can then be determined. Since $\hat{R}/\hat{H}$ is known from steady state creep data, individual values for $\hat{R}$ and $\hat{H}$ can then be found. Further, by making use of the second and third of equations (32), the parameters R and H then are known. Finally, the viscoplastic parameters $Y_L(\equiv K_T(4\omega^2 - 1)^{1/2})$, μ, n, m, β, R, and H are completely determined, as are the measures of the strength of transverse isotropy, ω and η.

SUMMARY AND CONCLUSIONS

A constitutive theory is presented to represent the high-temperature, time-dependent, hereditary behavior of materials that can be idealized as

initially transversely isotropic. In particular, the theory is applicable to metal matrix composite materials at elevated temperature where their mechanical behavior includes significant viscoplasticity (e.g., creep, relaxation, thermal recovery, etc.) and, at the same time these materials are strongly directional. It is presumed that a single preferential (fiber) direction is identifiable at each material point thereby admitting the idealization of local transverse isotropy. Although not addressed here, the theory can be extended, at the expense of some additional complexity, to account for two (or more) identifiable preferential directions at each material point.

The composite is viewed as a continuum in its own right; and detailed interactive effects of the constituents are not accounted for directly. Of course, this precludes predictions of detailed phenomena such as failure by debonding, delamination, and so forth. However, the result is a reasonably simple multiaxial constitutive theory that is easily implemented into structural analysis codes for predicting the deformation response of structures subjected to complex thermomechanical loading histories. Because the response in the presence of material anisotropy is often highly nonintuitive, this theory provides a valuable tool for the design engineer.

Some fundamental aspects of the theory are explored through geometric interpretation of some basic features analogous to those of time-independent plasticity theory. Convexity of the dissipation potential surfaces (F = constant or Ω = constant) is demonstrated, and the shape of the surfaces is shown to be dependent on the strength and orientation of anisotropy. An example involving the response of a thin-walled tube under internal pressure demonstrates the qualitative changes in the inelastic deformation mode that can result from directional strengthening (anisotropy).

A key ingredient in the present work is the specification of an experimental procedure for the complete determination of the material parameters for a particular metal matrix composite. The parameters relating to the strength of anisotropy are determined through probing experiments on thin-walled tubes of two kinds; circumferentially reinforced (a single fiber direction oriented circumferentially) and longitudinally reinforced (axial fiber direction). The tubes are loaded in both tension and torsion. The parameters relating to the viscoplastic properties of the composite are determined primarily through uniaxial creep tests conducted on longitudinally reinforced tubes. Alternately, as discussed, one could use pure torsion tests on circumferentially reinforced tubes in place of the uniaxial creep tests. Additional tests are suggested in order to assess the correctness and accuracy of the theory.

REFERENCES

1. Chamis, C.C.: Simplified Composite Micromechanics Equations for Hygral, Thermal and Mechanical Properties. SAMPE Q., vol. 15, no. 3, Apr. 1984, pp. 14-23.

2. Chamis, C.C.; and Hopkins, D.A.: Thermoviscoplastic Nonlinear Constitutive Relationships for Structural Analysis of High Temperature Metal Matrix Composites. NASA TM-87291, 1985.

3. Petrasek, D.W.; and Signorelli, R.A.: Tungsten Fiber Reinforced Superalloys - A Status Review. Ceram. Eng. Sci. Proc., vol. 2, nos. 7-8, 1981, pp. 739-786.

4. Westfall, L.J., et al.: Preliminary Feasibility Studies of Tungsten/Niobium Composites for Advanced Space Power Systems Applications. NASA TM-87248, 1986.

5. McDanels, D.L.; Serafini, T.T.; and DiCarlo, J.A.: Polymer, Metal, and Ceramic Matrix Composites for Advanced Aircraft Engine Applications. NASA TM-87132, 1985.

6. Robinson, D.N.: Constitutive Relationships for Anisotropic High-Temperature Alloys. Nucl. Eng. Des., vol. 83, no. 3, 1984, pp. 389-396.

7. Rice, J.R.: On the Structure of Stress-Strain Relations for Time-Dependent Plastic Deformations in Metals. J. Appl. Mech. vol. 37, no. 3, Sept. 1970, pp. 728-737.

8. Ponter, A.R.S.; and Leckie, F.A.: Constitutive Relationships for Time Dependent Deformation of Metals. J. Eng. Mater. Technol., vol. 98, no. 1, Jan. 1976, pp. 47-51.

9. Ponter, A.R.S.: Convexity and Associated Continuum Properties of a Class of Constitutive Relationships. J. Mec., vol. 15, no. 4, 1976, pp. 527-542.

10. Robinson, D.N.: A Unified Creep-Plasticity Model for Structural Metals at High Temperature. ORNL/TM-5969, 1978.

11. Duffy, S.: A Viscoplastic Constitutive Theory for Transversely Isotropic Metal Alloys. Ph.D. Dissertation, University of Akron, 1986.

12. Lance, R.H.; and Robinson, D.N.: Limit Analysis of Ductile Fiber Reinforced Structures. J. Eng. Mech. Div. Am. Soc. Civ. Eng., vol. 98, no. EM1, Feb. 1972, pp. 195-209.

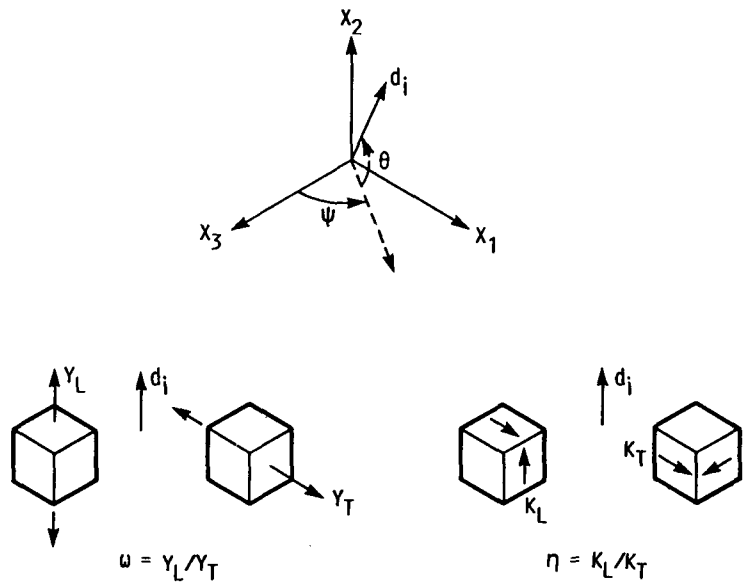

FIGURE 1. - PARAMETERS ACCOUNTING FOR TRANSVERSE ISOTROPY ψ, θ, ω, η. THE LOCAL FIBER DIRECTION IS DENOTED BY THE UNIT VECTOR d_i - SPECIFIED BY THE EULER ANGLES ψ AND θ. Y_L, Y_T, K_L, AND K_T ARE THRESHOLD STRESSES AS INDICATED. DEFINITIONS OF THE PARAMETERS ω AND η ARE GIVEN.

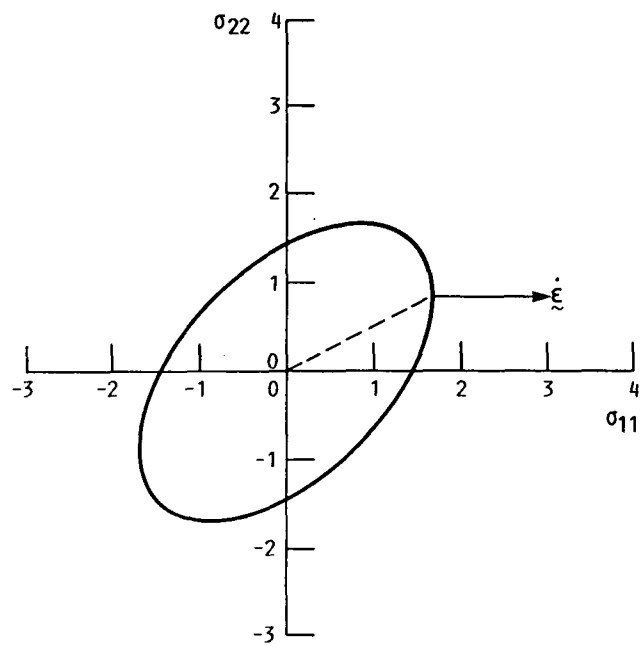

FIGURE 2. - PROJECTION OF FLOW SURFACE $F = 0$ ON σ_{11}-σ_{22} PLANE ($\omega = \eta = 1$-ISOTROPY). UNITS OF STRESS ARE ARBITRARY.

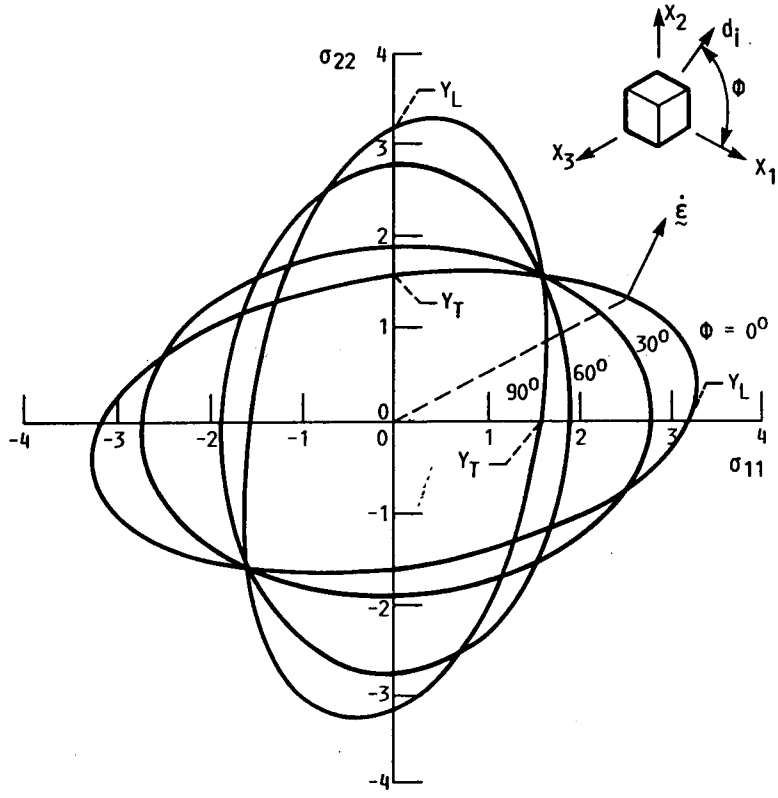

FIGURE 3. - PROJECTION OF FLOW SURFACES F = 0 ON σ_{11}-σ_{22} PLANE ($\omega = \eta = 2$). UNITS OF STRESS ARE ARBITRARY.

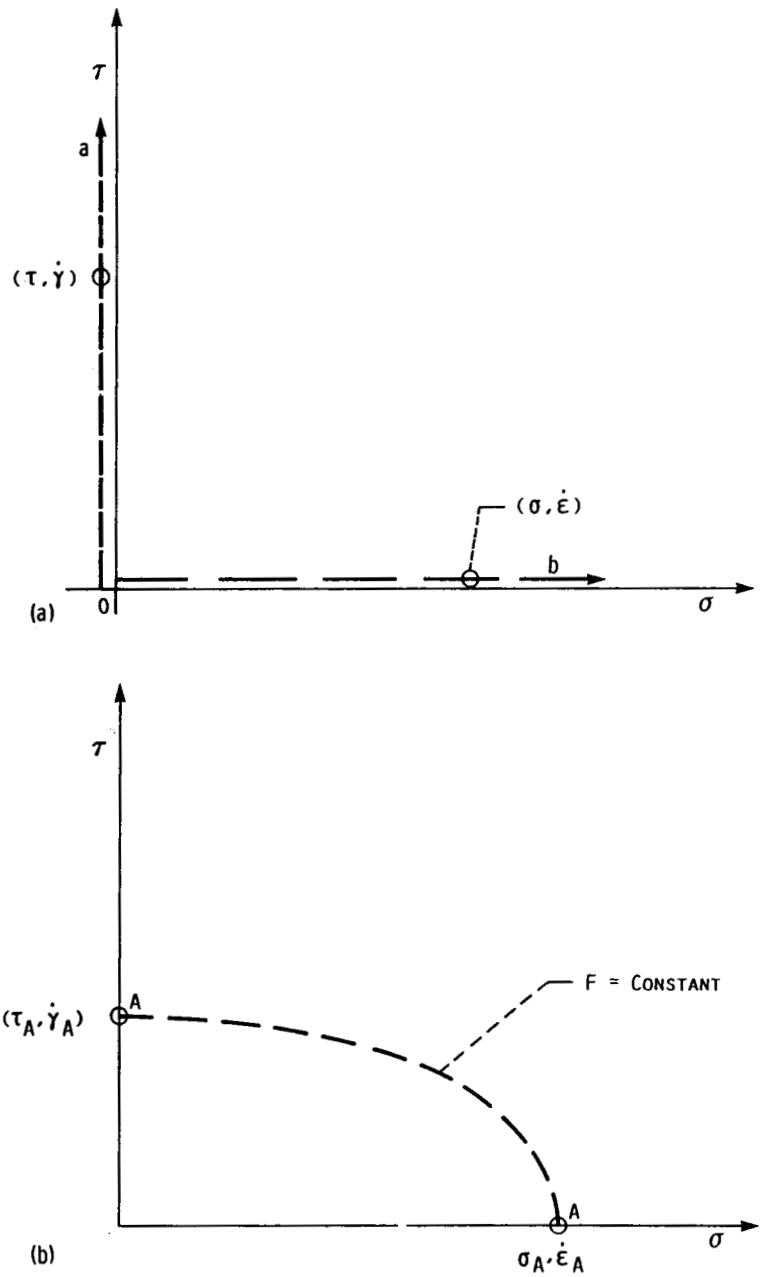

FIGURE 4(a). - TENSION AND TORSION PROBES SCHEMATICALLY ILLUSTRATED IN THE σ-τ STRESS PLANE.
4(b). - DATA POINTS THAT LIE ON A COMMON F = CONSTANT CURVE. POINTS A,A HAVE THE SAME DISSIPATION RATE.

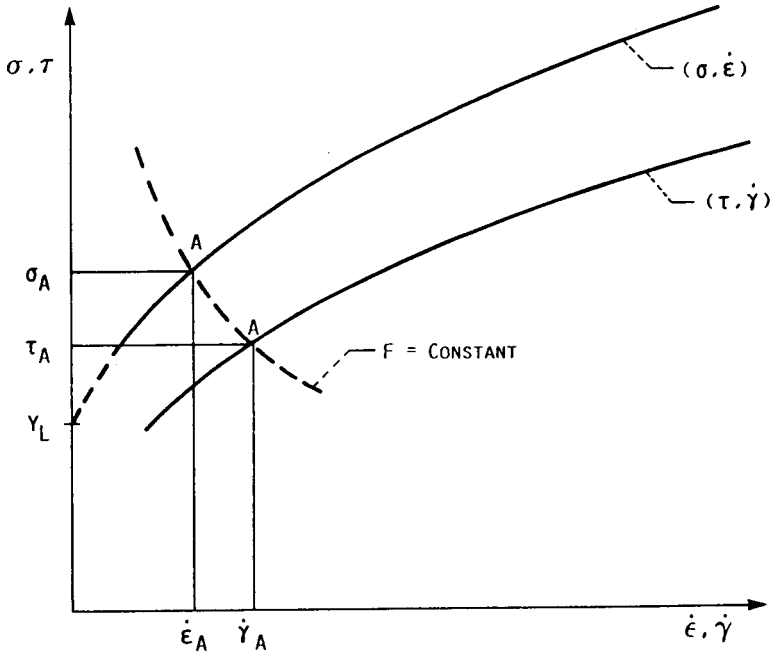

FIGURE 5. - STRESS AND INELASTIC STRAIN RATE PAIRS FROM TORSION AND TENSION PROBE DATA ON A LONGITUDINALLY REINFORCED TUBE.

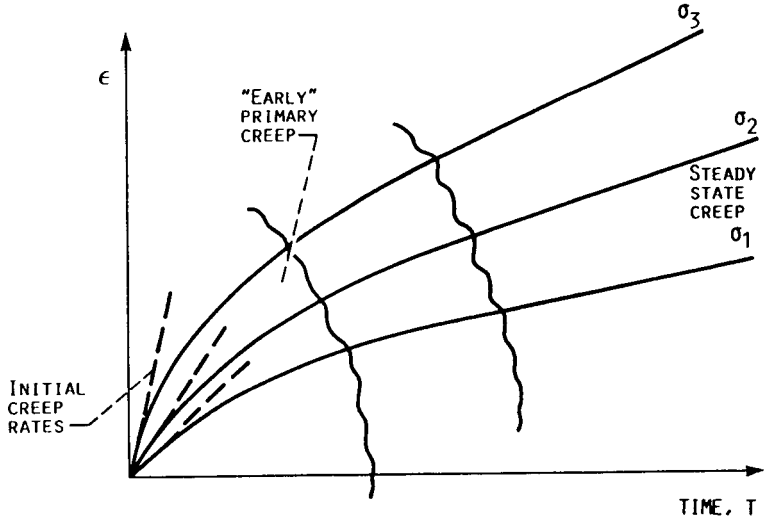

FIGURE 6. - TYPICAL CREEP CURVES.

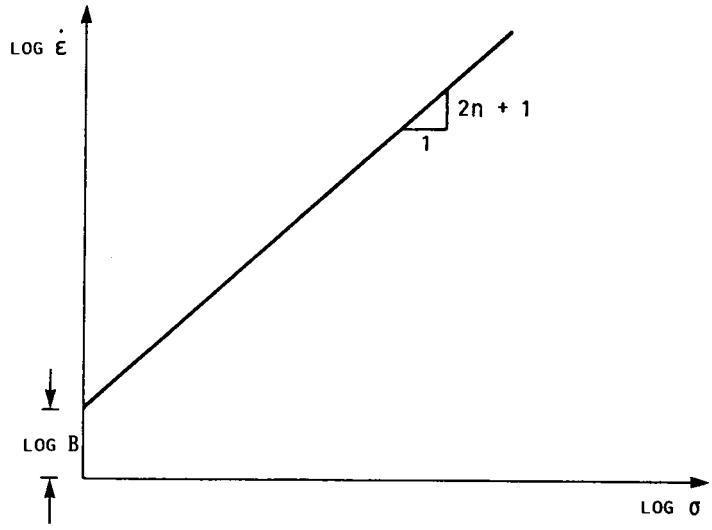

FIGURE 7. - DETERMINATION OF B AND n.

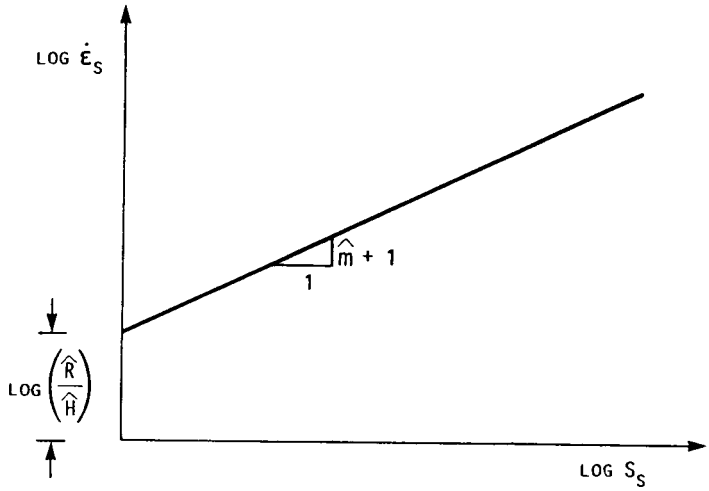

FIGURE 8. - DETERMINATION OF $\hat{m}$ AND $\hat{R}/\hat{H}$.

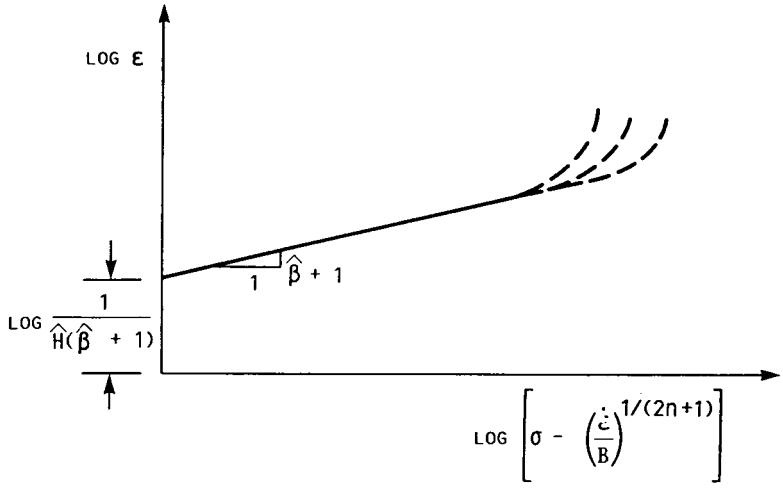

FIGURE 9. - DETERMINATION OF $(\hat{\beta} + 1)$ AND $1/\hat{H}(\hat{\beta} + 1)$.